ELSEVIER

Polymer 42 (2001) 5925–5935

polymer

www.elsevier.nl/locate/polymer

The evolution of structure and properties in poly(*p*-phenylene terephthalamide) fibers

Y. Rao, A.J. Waddon, R.J. Farris*

Polymer Science and Engineering Department, University of Massachusetts Amherst, Amherst, MA 01003, USA

Received 1 May 2000; received in revised form 1 December 2000; accepted 6 December 2000

Abstract

The evolution of the mechanical properties and structure of poly(*p*-phenylene terephthalamide) (PPTA) fibers with different post-treatment methods involving heat, tension, hydrostatic pressure, and different environments was systematically investigated. Wide-angle X-ray diffraction measurements reveal that the crystal structure of PPTA fiber is not stable and changes upon post-treatment. The cooperative changes in the modulus and two structure parameters — the misorientation angle and the paracrystalline parameter upon treatment — indicate a direct structure–property correlation. After studying free-length annealing and heat-tensioning of fibers, several structure parameters — the *c*-dimension of lattice constants, the paracrystalline parameter, the intensity ratio between (110) and (200), and the orientation angle — were found to be affected greatly by the tension applied during heat stretching; while other structure parameters such as apparent crystal sizes, equatorial crystallinity and *a*, *b* dimensions of the lattice constant are insensitive to the applied tension but determined by the applied temperature and time. A sudden change in the crystal structure at 400°C suggests a α-relaxation in the crystalline region, which is supported by the DMTA and TMA measurements.

Keywords: Poly(*p*-phenylene terephthalamide) Kevlar® fibers; Structure and properties; Wide-angle X-ray diffraction

1. Introduction

Poly(*p*-phenylene terephthalamide) (PPTA) fiber is known to have very high modulus and strength and good thermal stability [1]. The property of the fiber can be greatly enhanced through post-treatment. In order to achieve better performance, it is important to understand what structure change is caused by post-treatment and how this structure change relates to the property enhancement. In recent years several studies were made on the structure–property relation [2–5]. However, no systematic study of the structure change upon treatment has been reported.

PPTA is a highly crystalline polymer [4,6–13]. A single-phase structure with crystalline imperfection describes its morphology well [9]. The crystal structure of PPTA shown by Northolt and Aartsen is a pseudo-orthorhombic [6,7]. Panar and coworkers suggested a paracrystalline structure of the crystal with a second order distortion g_{II} of 2.5% along *c*-axis [9]. These imperfect crystals are packed to form pleated sheets and those pleats can be observed using polarized optical microscopy [5,8,14,15].

Wu et al. [14] studied the crystal structure change of PPTA fiber under annealing temperatures ranged from 380 to 480°C at either no-tension or constant-tension modes. They proposed a residual-stress free *c*-dimension of a crystal. Then, an increase in *c*-dimension was observed for all treatments. The higher the tension, the bigger the increment is; and the higher the annealing temperature, the smaller the increment. They also discussed the change in the apparent crystal size along *c*-axis and the degree of orientation. Lee and coworkers did a similar study on the structure and property development of PPTA during heat treatment under tension [5]. They observed a correlation between the modulus and the orientation as well as the pleating. Other structure parameters such as crystal size and paracrystallinity were found to be irrelevant to the property. It was reported that the fiber tenacity does not change much at low and intermediate temperatures for short time annealing but drops when the temperature exceeds 450°C and degradation occurs [8]. Several hours' exposure to high temperature deteriorates the strength but does not affect the modulus much [15]. The crystallites were found to grow laterally along the *b*-axis upon thermal annealing [16].

Different researchers have focused exclusively on certain structure parameters, narrow range of treatment temperature or specific method in their study of the structure change

* Corresponding author. Tel.: +1-413-577-3125; fax: +1-413-545-0082.
E-mail address: rjfarris@polysci.umass.edu (R.J. Farris).

0032-3861/01/$ - see front matter
PII: S0032-3861(00)00906-X

Table 1

	Temperature (°C)	Time (mins)	Tension (MPa)	Hydrostatic pressure (MPa)	Media
Free length annealing	Varied 180–500	180	0	0	N_2
Tensioning annealing	Varied 180–370	3	Varied	0	N_2
Pressure tensioning annealing	250	1.5	800	90	Silicone oil
Pressure steam annealing	Varied 100–300	120	0	Saturated steam	H_2O
Pressure annealing	260	240	0	130	Mercury

upon post-treatment. In this paper, the change in the properties and structure of PPTA fibers was studied in a wide range of temperature from 180 to 500°C. In addition, different post-treatment conditions including tension, hydrostatic pressure with inert gas or water were utilized. Then all relevant structure parameters were investigated. Our experiments disclose the instability of the crystal structure of PPTA and a α-relaxation around 400°C in the crystalline region. Our results strongly indicate the modulus of the fiber is determined by the combination of the orientation and the paracrystalline parameter.

2. Experimental

One thousand five hundred denier yarns of Kevlar® 119, Kevlar® 29, Kevlar® 49 and Kevlar® 149 fibers were supplied by DuPont. Five different post-treatment methods were used to alter the properties and structure of the fiber:

1. free length annealing where fiber yarns were placed inside a glass container loosely and put in an oven with nitrogen purge at set temperature;
2. tensioning annealing where fiber yarns were put through a homemade heat-treatment apparatus and then a dead weight was hung for constant tension with a mobile oven to control the heating time;
3. pressure-tensioning annealing where fiber yarns were sealed in the same homemade heat-treatment apparatus and pretension was controlled by a tension-control device with silicone oil as the pressurizing agent;
4. pressured steam annealing where fiber yarns were put in a heatable high pressure vessel and certain amount of water was injected to achieve saturated water/steam at heat treatment temperature;
5. pressure annealing where a P–V–T rig was used to hold the sample and mercury was used as the pressurizing agent.

The conditions explored are listed in Table 1.

The methods of property and structure measurements were described in detail in another paper [17]. To gain better statistics, yarn tests were conducted. Single filament tests were used only when yarn samples were not available. At least three samples were tested for one condition. The mechanical properties were measured by an Instron® and MTS® tester. The initial modulus, which is the modulus in the strain range of 0.1–0.5%, the strength and the break strain were recorded. The structure was characterized using wide-angle X-ray diffraction. The structure parameters investigated include lattice constants, a, b, c; paracrystalline parameter, g_{II}; equatorial X-ray diffraction crystallinity, X; intensity ratio, I_{110}/I_{200}; different apparent crystal sizes (ACS) of planes (00l), (110) and (200); and the (200) orientation angle, $\phi_{200,x}$. Simens® D500 diffractometer, Simens® two-dimensional area detector and Statton® Camera were used.

Table 2 [17] lists the statistics of different measurements for structure characterization and error bars will not be included in Section 3.

Dupont TMA 2950 and Rheometric Mark IV DMTA were used for thermomechanical measurements.

3. Results and discussion

Table 3 summaries the properties and structure parameters of the post-treated fibers.

Table 2

	Lattice constant (Å)	Paracrystalline parameter g_{II} (%)	Equatorial crystallinity X (%)	Intensity ratio I_{110}/I_{200}
Standard deviation[a]	0.003	0.04	4	0.03
	Apparent crystal size		(200) orientation angle (°)	
	(110), (200) nm	(00l), nm		
Standard deviation[a]	0.2	7	0.3	

[a] Listed numbers are the maximum standard deviation in the measurement of different samples.

Table 3
Datasheet of the annealing of Kevlar® fiber (treatment time unless otherwise noted: 3 h)

Treatment condition			Property			Structure									
Temperature (°C)	Tension (GPa)	Condition	Modulus (GPa)	Tenacity (GPa)	Strain to break (%)	Lattice constant			g_{II}[a] (%)	X[b] (%)	I_{110}/I_{200}[c]	Apparent crystal size			$\phi_{200,x}$ (°)
						a (Å)	b (Å)	c (Å)				(002) nm	(110) nm	(200) nm	
Free-length annealing															
Kevlar® 29 as spun			78	2.58	3.1	7.75	5.23	12.838	1.92	76	0.70	656	52	46	12.2
180	0	N_2	78	2.28	3.1	7.81	5.23	12.838	1.81	75	0.69	735	61	48	12.8
200	0		78	2.2	3.1	7.81	5.23	12.838	1.78	77	0.67	734	63	48	13.0
250	0		77	1.68	2.4	7.84	5.22	12.836	1.72	72	0.67	920	71	52	13.6
300	0	2 h	78	1.55	2.2	7.86	5.21	12.840	1.68	74	0.66	800	77	54	13.1
300	0		75	1.65	2.3	7.87	5.22	12.852	1.74	77	0.65	815	80	56	14.0
350	0		71	1.2	2.11	7.86	5.21	12.852	1.70	74	0.67	820	84	59	14.7
350	0	10 h	76	1.1	2	7.96	5.20	12.854	1.70	76	0.73	500	85	61	14.3
400	0		56	0.54	0.9	7.87	5.20	12.824	1.91	74	0.77	418	90	63	15.0
450	0	15 min	66	0.83	1.55	7.87	5.20	12.830	1.99	72	0.75	400	82	60	14.6
450	0	30 min	61	0.4	0.92	7.87	5.18	12.830	1.80	70	0.75	321	85	62	15.8
450	0	45 min	60	0.21	0.6	7.85	5.19	12.800	1.89	70	0.75	221	86	62	15.1
450	0		40	0.1	0.5	7.85	5.18	12.718	2.13	60	0.75	154	86	62	20.9
500	0	10 h	42	0.05	0.2	7.88	5.19	12.740	2.38	41	0.87	150	93	68	21.0
Kevlar® 119 as spun			61	2.96	4.10	7.75	5.22	12.820	1.91	75	0.74	609	50	45	16.2
450	0	15 min	55	0.87	1.58	7.87	5.19	12.820	1.88	75	0.66	650	91	66	17.7
450	0	30 min	49	0.48	0.8	7.87	5.19	12.820	1.94	75	0.70	735	61	66	18.0
450	0	45 min	50	0.21	0.4	7.87	5.19	12.820	2.06	75	0.72	450	92	67	18.1
Kevlar® 49 as spun			113	2.40	2.47	7.78	5.23	12.880	1.66	77	0.61	737	66	51	6.8
450	0	30 min	90	0.82	0.9	7.88	5.19	12.870	1.75	69	0.68	700	95	67	9.8
Kevlar® 149 as spun			138	2.15	1.50	7.90	5.19	12.920	1.40	77	0.60	1548	123	76	6.4
450	0	15 min	120	0.24	0.2	7.87	5.18	12.910	1.50	99	0.63	1500	125	80	7.2
Kevlar® 29, heat tension															
180	0.92	3 min	105	2.45	2.5	7.81	5.23	12.880	1.65	77	0.56	700	64	50	8.2
180	1.2	3 min	108	2.4	2.4	7.81	5.23	12.880	1.60	77	0.52	658	65	50	
180	1.5	3 min	116	2.39	2.42	7.81	5.23	12.888	1.55	77	0.48	730	65	50	6.9
230	1.2	3 min	110	2.38	2.44	7.84	5.22	12.890	1.57	77	0.51	800	75	53	8.7
230	1.5	1.5 min	113	2.38	2.2	7.84	5.22	12.880	1.68	77	0.48	850	75	53	7.2
370	0.76	1 min	140	2.25	1.53										
Kevlar® 29, pressure–heat–tension															
250	<0.8, 1 min	90 MPa, SiO_2	80	2.5	2.9	7.75	5.23	12.852	1.87	72	0.65	1800	57	50	10.7
260	0	130 MPa Hg	101	0.25	0.3	7.77	5.22	12.846	1.99	80	0.71	1800	79	62	8.2
Kevlar® 29, pressurized steam															
100	0	0.1 MPa	78	2.2	2.4	7.75	5.23	12.838	1.93	77	0.70	658	55	48	12.2
204	0	1.1 MPa	78	1.85	2.05	7.75	5.23	12.838	1.95	75	0.74	1500	61	45	11.9
300	0	9.8 MPa	92	1.75	2.1	7.75	5.23	12.838	2.04	71	0.67	600	64	51	11.3

[a] Paracrystalline parameter.
[b] Equatorial crystallinity.
[c] Intensity ratio of two diffraction peaks.

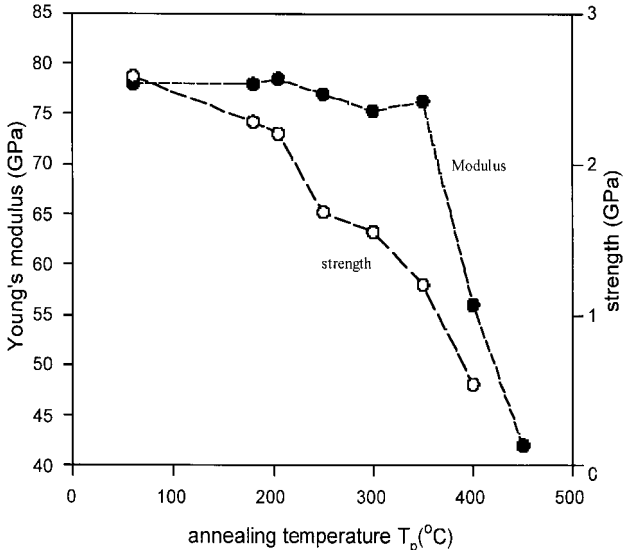

Fig. 1. Properties of the fiber under different annealing temperatures in free-length annealing: close circles are modulus and open circles are strength.

3.1. Free length annealing

3.1.1. Mechanical properties

Upon free length annealing, the modulus of Kevlar® 29 fiber decreases slightly with the annealing temperature until 400°C and then drops rapidly as shown by Fig. 1. The strength of the fiber starts to deteriorate when the annealing temperature is higher than 250°C. After being annealed at 450°C for 30 min, the modulus drops by 46% and the strength decreases by 80%. The color of the fiber also becomes darker when the annealing temperature is above 400°C. This result is similar as annealing effect on Kevlar® 49 observed by Hindeleh [4].

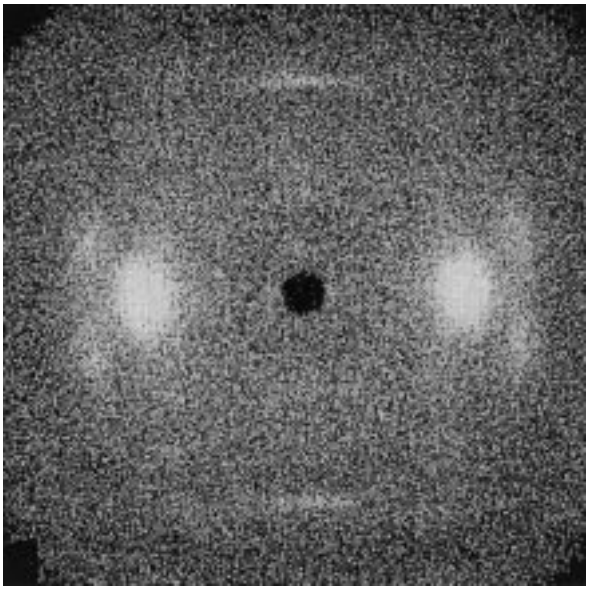

Fig. 2. WAXD pattern of Kevlar® 29 fiber.

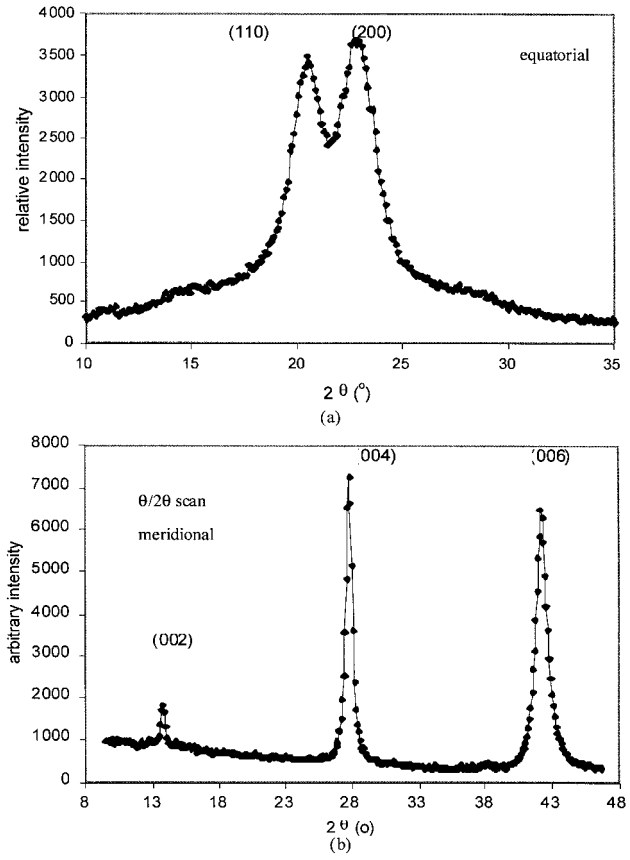

Fig. 3. Typical diffraction scans for Kevlar® fiber: (a) equatorial scan; (b) meridional scan.

3.1.2. Lattice parameters

A typical diffraction pattern of Kevlar® fiber is shown in Fig. 2. Its corresponding meridional and equatorial scans are shown in Fig. 3.

The lattice constants of PPTA crystal has been carefully examined by wide angle X-ray diffraction. The high orientation of PPTA fiber makes the measurement of lattice *c*-dimension difficult. The sample was tilted at certain angle to allow *c*-axis to intercept with the Ewald sphere. The *c*-dimension was calculated from the regression of three orders of meridional diffraction as illustrated in Fig. 4. It was found that the *c*-dimension of PPTA crystal changes upon annealing. Fig. 5 shows that the *c*-dimension is relatively constant when the annealing temperature is lower than 250°C. Then the *c*-dimension increases with the annealing temperature until 350°C and decreases rapidly afterwards. This discloses that the crystal structure of PPTA is not thermally stable. This is not difficult to understand. Because PPTA is a lyotropic liquid crystalline polymer, the ordered structure can be formed from the liquid crystal state. This ordered structure is probably frozen via coagulation and is not an equilibrium state. Therefore any post-treatment serves as an evolution in the crystal's metastable state. As the strong intramolecular

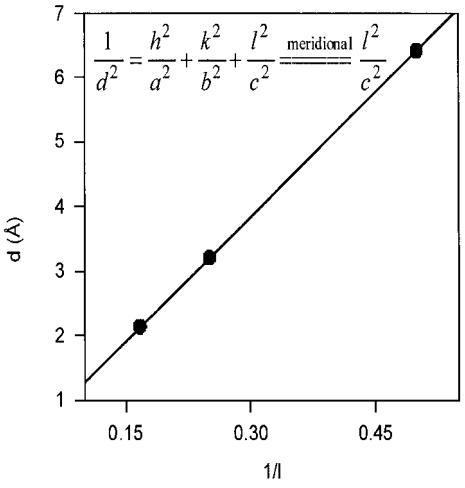

Fig. 4. Calculation of c from several orders of meridional diffraction.

interaction overcomes the weaker intermolecular forces, namely hydrogen bonding and van der Waals force in the case of PPTA, a polymer crystal is merely the packing of chains. Hence, the external force can apply directly to the chain and the crystal dimension is changed due to the deformation of a single chain. This structure instability was also observed by Haraguchi and coworkers in their study on the PPTA film [18]. Haraguchi attributed that instability to the metastable crystal form II of PPTA film made by coagulating with water. Our study shows that the instability of PPTA crystals is more general. A thermal expansion experiment was conducted in order to compare the microscopic permanent deformation with the macroscopic deformation. Fig. 6 is the thermal expansion curve of Kevlar® 29 as spun fiber. There is a resemblance between the change of c-dimension measured by X-ray diffraction and the thermal expansion coefficient with the annealing temperature. Therefore, the change in thermal expansion coefficient α well represents the structural change in the material due to high temperature annealing.

There are also slight changes in a-, b-lattice dimensions. Fig. 11(c) reveals that the a-dimension increases with

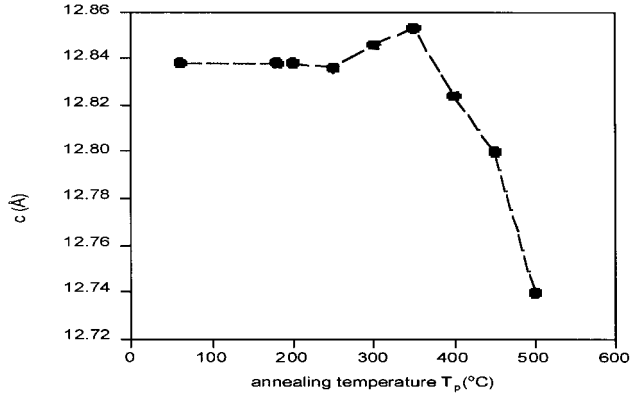

Fig. 5. Change of the lattice c-dimension with the annealing temperature in the study of free-length annealing.

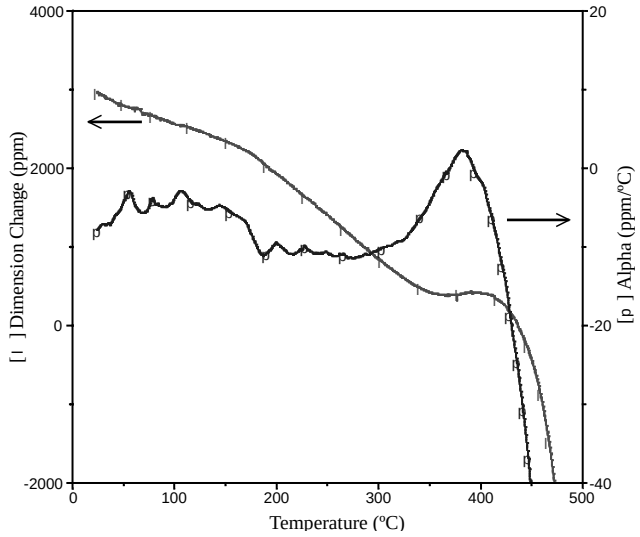

Fig. 6. Dimension change of Kevlar® 29 as spun fiber upon heating: close symbols are dimension and open symbols are linear thermal expansion coefficient α; heating rate: 10°C/min.

annealing temperature while b-dimension decreases. The crystal structure change with the annealing temperature lower than 350°C can be represented by Fig. 7. In PPTA crystal, hydrogen bonding is along b-direction and van der Waals force along a-direction. There is water bound to the polymer chain through hydrogen bonding when fiber is coagulated. Upon heating, this bound water is removed and gives mobility to the chains to form more hydrogen bonds between them. Therefore, the b-dimension is shortened.

3.1.3. Paracrystalline structure

The imperfection of PPTA crystal is found to be described by the paracrystals [3,9,10]. The concept of paracrystals was first introduced by Hosemann [19]. Three parameters of the dimension of the unit cell, the electron-density distribution within the cell and the crystal size can characterize an ideal crystal. If the dimension of the unit cell and the electron-density distribution vary statistically from cell to cell, a paracrystallinity is needed. As in PPTA fiber, a conformational distribution can cause the paracrystallinity. Therefore, the information of paracrystalline structure will be very helpful in understanding the deformation

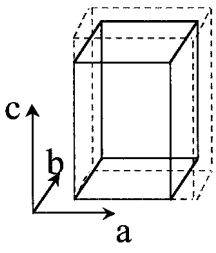

Fig. 7. Change of the unit cell upon annealing: solid line: as spun and dash line: annealed.

mechanism under different loading modes. The broadening effect in a paracrystal can be described by the following equation:

$$(\delta s)_0^2 = (\delta s)_c^2 + (\delta s)_{II}^2 = \frac{1}{\bar{L}_{hkl}^2} + \frac{(\pi g_{II})^4 m^4}{d_{hkl}^2}$$

in which δs is the broadening of the diffraction peak, $\bar{L}$ the crystal size, g_{II} the paracrystalline parameter, m the order of the diffraction peak, d_{hkl} the dimension of the first order diffraction plane.

A typical plot between the peak width and the diffraction order for PPTA crystal is shown in Fig. 8 and its paracrystalline parameter g_{II} can be calculated accordingly. The paracrystalline parameter of PPTA fiber was found to change with the annealing temperature as shown in Fig. 9. The paracrystalline parameter first decreases with the annealing temperature and increases rapidly when the annealing temperature is higher than 350°C. Fig. 9 also shows that the intensity ratio of the diffraction peak of (110) to (200) changes similarly as the paracrystalline parameter. The I_{110}/I_{200} was shown to be an important structure aspect in studying the structure change due to water desorption, although the nature of this ratio remains unclear [20]. Both Figs. 5 and 9 show two transitions at 250 and 350°C, respectively. This tells us that several structure parameters — the lattice *c*-dimension, the paracrystalline parameter and the intensity ratio of I_{110}/I_{200} — undergo a cooperative change when the material is annealed. The analysis of the change of these three parameters yields a nonlinear chain model to describe the paracrystal in PPTA [17]. Upon heating, the molecular chain tends to move to more extended conformation, which may involve the transformation of *gauche* to *trans* conformation. Then when the temperature reaches 350°C, there is big decrease in lattice *c*-dimension due to the gained mobility. In addition, these structure changes are frozen by cooling because of the long relaxation time.

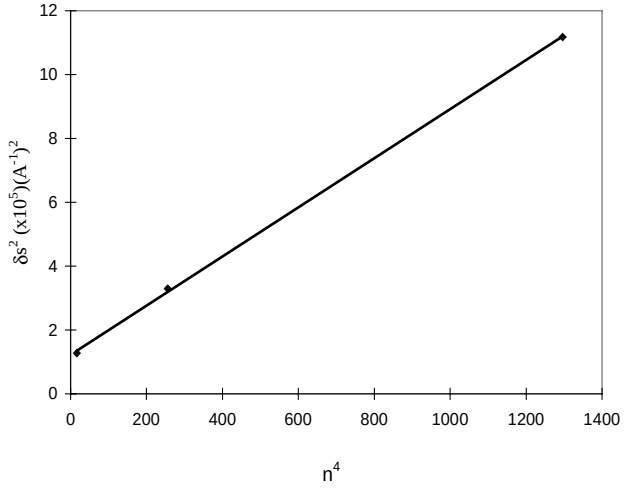

Fig. 8. The square of the peak breadth vs. the fourth power of the reflection order describing paracrystalline disorder in Kevlar® 29.

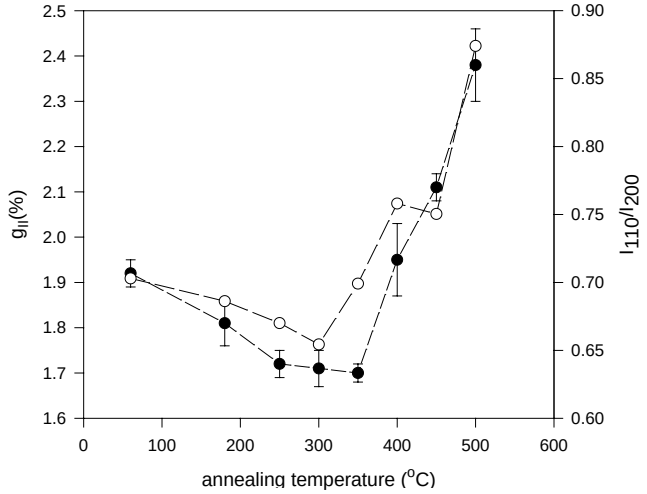

Fig. 9. Paracrystalline parameter g_{II} and intensity ratio I_{110}/I_{200} under different annealing temperatures in the study of free-length annealing: close circles are g_{II} and open circles are I_{110}/I_{200}.

The thermal study of PPTA fiber is difficult to conduct and rare. Hindeleh and Abdo concluded that PPTA has a glass transition at 370°C from DTA trace [4]. Our result suggests that the structure of PPTA gain certain mobility around 350°C. The big change in the crystal structure at 350°C indicates that the local rearrangement happens within or on the surface of the crystalline region. The transition at 350°C may be attributed to α-relaxation in the crystalline region and the transition at about 200°C is β-relaxation in the crystalline region. It is possible that the mobility is enhanced by the relaxation in the amorphous phase if there is such content existing in the PPTA. To further study the relaxations in PPTA fiber, DMTA measurements were performed. Fig. 10 is a DMTA spectrum of a Kevlar® 29 as spun single filament. Three peaks appear in its tanδ trace. The first peak associates with the removal of water

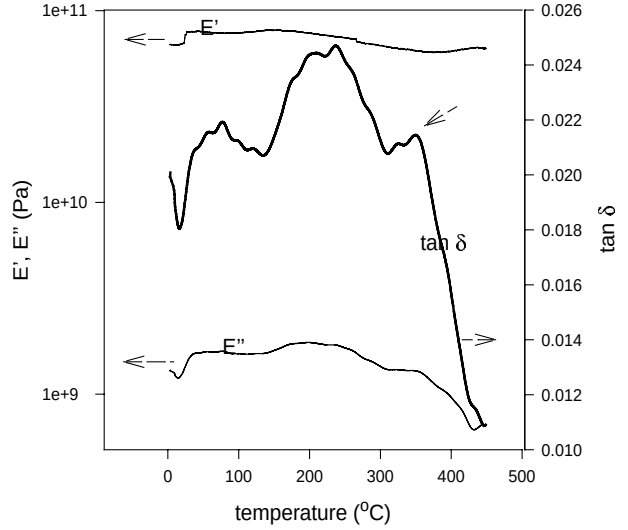

Fig. 10. DMTA spectrum of Kevlar® 29 as spun fiber: heating rate, 5°/min.

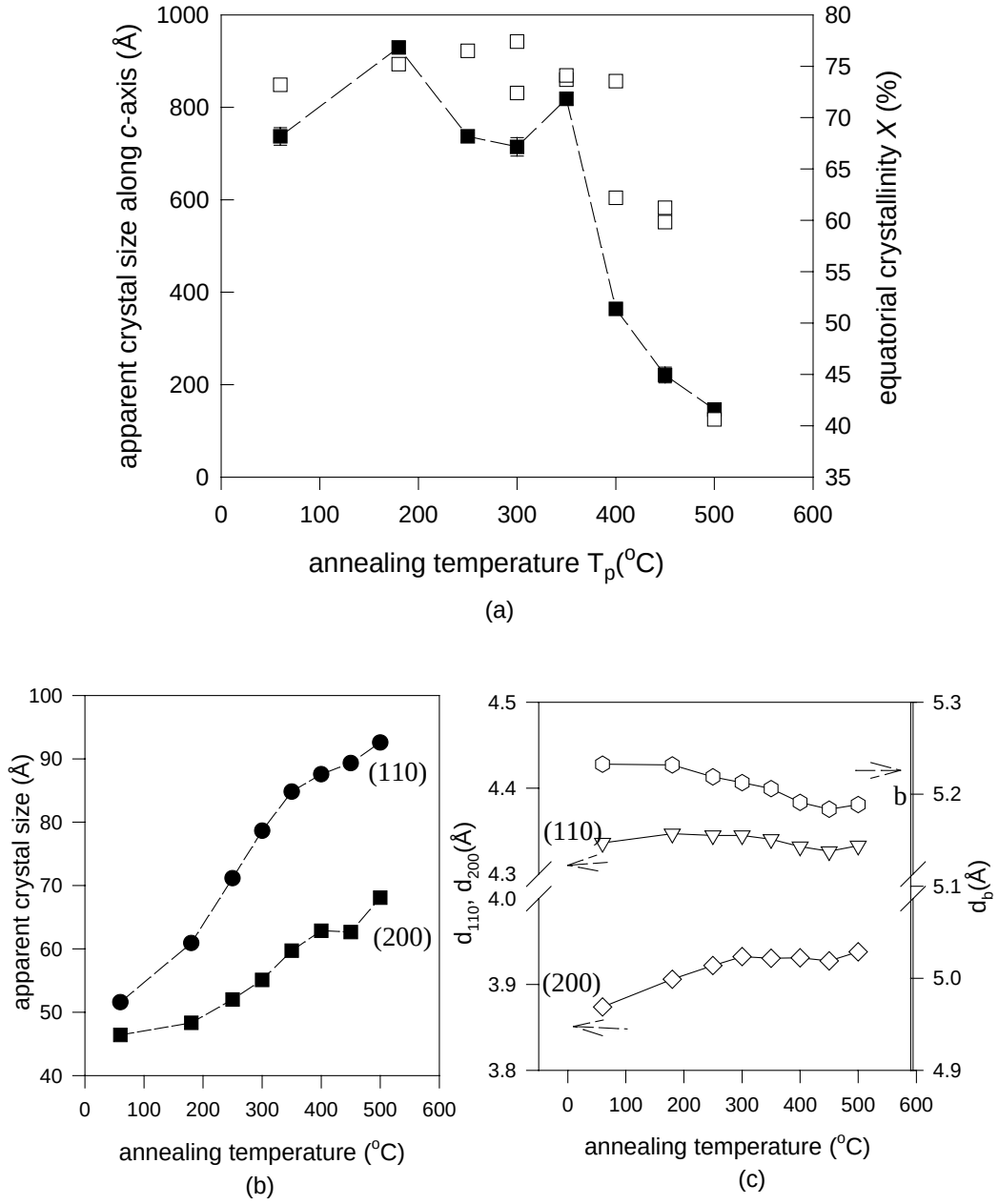

Fig. 11. Change of the transverse structure of the crystal in Kevlar® 29 fiber with the annealing temperature in free-length annealing: in plot (a) close symbols are the apparent crystal size along *c*-axis and open symbols are equatorial crystallinity *X*; (b) transverse apparent crystal sizes; (c) transverse lattice constants.

from the intercrystalline region and the crystal structure remains unchanged. The second and third peaks correspond well to the transitions observed by X-ray diffraction.

3.1.4. Apparent crystal sizes (ACS)

Heat annealing can largely change crystal sizes. Fig. 11(b) shows that the apparent crystal sizes of (110) and (200) increase monotonically with the annealing temperature. The apparent crystal size of (110) increases faster than (200). This was also observed by other researches [4,20,21]. However, Hindeleh and Abdo reported differently that the transverse apparent crystal sizes decrease when the annealing temperature is higher than 400°C.

Fig. 11(a) shows that the apparent crystal size along *c*-axis does not change with the annealing temperature until 350°C after which the apparent crystal size along *c*-axis starts to decrease. Fig. 11(a) also includes the effect of the annealing temperature on equatorial crystallinity. The change in the equatorial crystallinity with the annealing temperature is similar to the change in the apparent crystal size along *c*-axis.

3.1.5. Orientation

When the modulus change due to free-length annealing is compared with the structure changes discussed, there is no good correlation. The reason is because of another

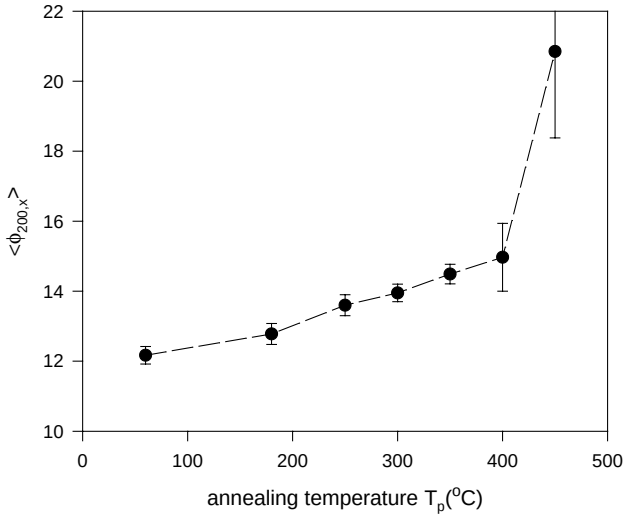

Fig. 12. Orientation angle $\phi_{200,x}$ under different annealing temperatures in free-length annealing.

important structure parameter in PPTA fiber: misorientation of the crystals. It is found that there is de-orientation when the annealing temperature increases and the orientation of the crystals deteriorates after 400°C as shown in Fig. 12. The modulus of the fiber is shown to be determined mainly by the misorientation of the crystals. Meanwhile, a careful analysis suggests that paracrystalline structure also contributes to the modulus of the fiber. Shown in another paper [17] the modulus of the fiber can be calculated from the orientation angle and the paracrystalline parameter of the crystals.

The free-length annealing at 450°C of other commercial Kevlar® fibers, Kevlar® 119, Kevlar® 49 and Kevlar® 149, were also performed. Table 3 shows that all different fibers have the same transverse lattice constants and apparent crystal sizes after annealing. Their orientation angle and

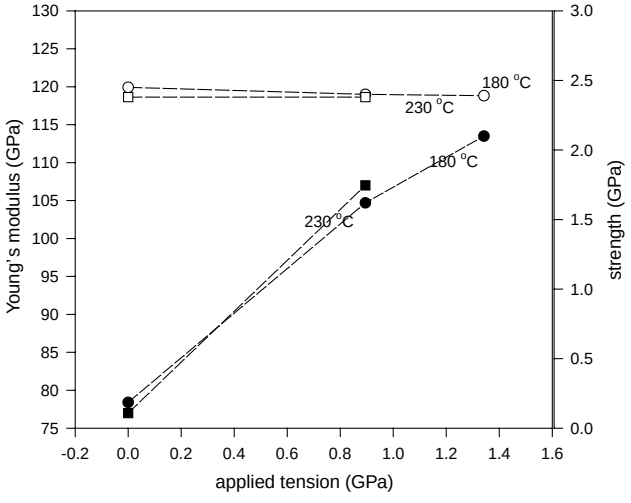

Fig. 13. Change of the properties of the fiber with applied tension in heat-tensioning: close circles are modulus and open circles are strength; numbers in the plot are treatment temperatures.

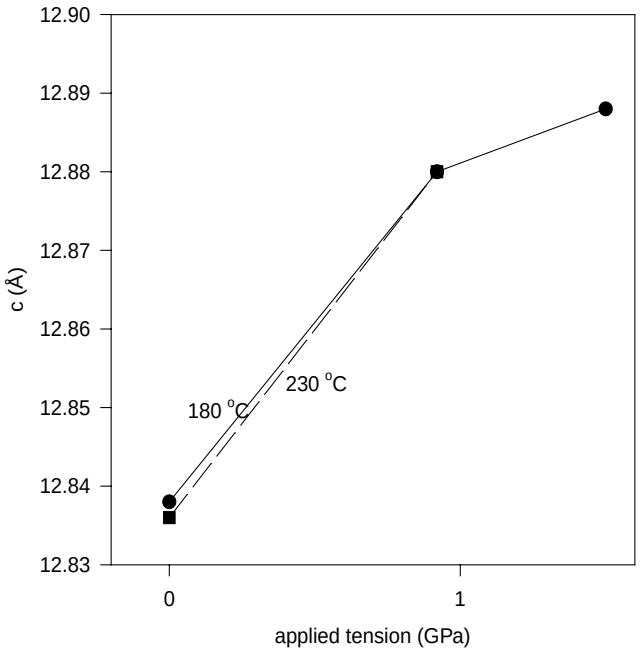

Fig. 14. Lattice *c*-dimension changing with applied tension in heat-tensioning; close circles are crystals treated at 180° and open circles are crystals treated at 230°.

paracrystalline parameter increase but are not the same after annealing.

3.2. Tensioning annealing

It is well known that PPTA fibers can be heat-treated under tension to improve the modulus. It is important to understand the structure change during this process.

It is illustrated in Fig. 13 that the modulus of the fiber can be greatly enhanced by the heat tensioning while its strength remains relatively unchanged. By applying a tension of 60% of its strength at elevated temperature, the modulus of the fiber can be increased by 50%. The increase in the modulus is almost linear with the applied tension at certain stretching temperature. The applied temperature does not have big effect on the increase in the modulus when the temperature is in certain range. However, the modulus is doubled when the fiber was treated at a much higher temperature (370°C).

The structure of the crystal and its packing are changed with the heat tensioning. The *c*-dimension of lattice constants increases with the applied tension at certain treatment temperature. (Fig. 14) Cooperatively, the paracrystalline parameter decreases as shown by Fig. 12. Fig. 15 also illustrates that the orientation angle decreases with the applied tension at certain treatment temperature. Corresponding to a modulus increase by 50%, the *c*-dimension increases by 0.4% and the orientation angle changes from 12.2 to 7.0°. The change in the orientation angle can cause a fiber to elongate by 1.5% if the crystal orientation contributes to the deformation. In our heat stretching experiments, a permanent deformation of 1.9% was observed when the

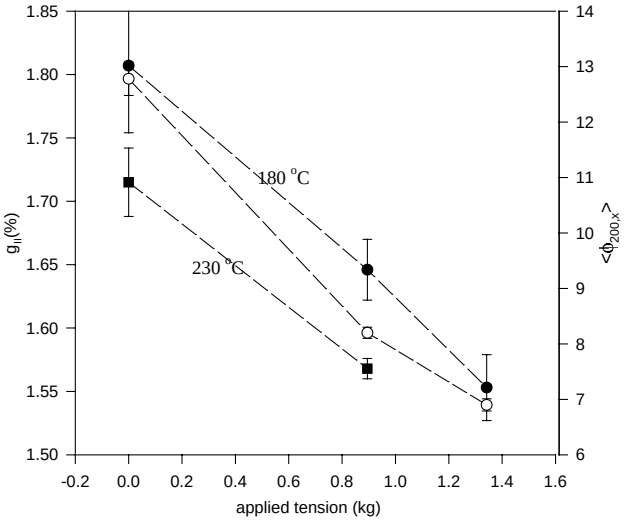

Fig. 15. Change of the paracrystalline parameter g_{II} and the orientation angle with applied tension in heat-tensioning: close circles are g_{II} and open circles are $\phi_{200,x}$; numbers in the plot are treatment temperatures.

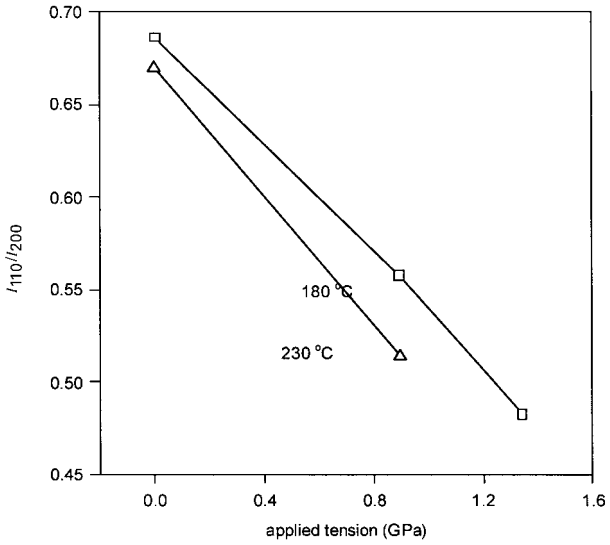

Fig. 16. Change of intensity ratio, I_{110}/I_{200}, with applied tension in heat-tensioning; numbers in the plot are treatment temperatures.

resultant fiber has a modulus increase of 50%. Therefore, the deformation of the fiber is caused by the combination of two mechanisms: the elongation and the rotation of the crystal. Our study supplements the deformation mechanism of crystal rotation for PPTA proposed by Ericksen [22].

It has been shown from the property–structure correlation [17] that the smaller the orientation angle and the paracrystalline parameter, the higher the modulus. The results of free-length annealing suggest that the orientation angle increases and the paracrystalline parameter decreases upon heating. A decrease in the paracrystalline parameter means the crystal becomes more perfect. This indicates that, naturally, crystals tend to de-orient while the crystal becomes more perfect upon heating. Because of the competition between two processes, the modulus of the fiber remains relatively unchanged at a wide range of annealing temperatures. When a tension is applied along heating and the tension is big enough to overcome the tendency of de-orientation of crystals and additionally force crystals to realign, the properties of the fiber can be improved due to two beneficiary effects, reorientation and perfection of the crystal as indicated in Fig. 13. This is the structure reason of the property enhancement by heat tensioning post-treatment.

Other structure changes were also observed. Fig. 16 indicates that the I_{110}/I_{200} decreases linearly with the applied tension. While they increase largely with the treatment temperature shown in the study of free-length annealing, the apparent crystal sizes are almost unchanged by the applied tension. The equatorial crystallinity does not change systematically with the applied tension. The lattice constants along *a*-, *b*-direction are also unchanged.

These structure characterizations clearly suggest that some structure parameters — the orientation angle, the lattice *c*-dimension, the paracrystalline parameter and the intensity ratio I_{110}/I_{200} — are closely related to the properties of the fiber, while the modulus of the fiber is insensitive to the *a*, *b*-lattice constants and apparent crystal sizes.

A heat-tensioning experiment at 370°C yields a fiber with a modulus increase by 100% while its structure characterization was not performed due to the small quantity of the sample (Table 3). This big-scale increase in the modulus could not be achieved by tensioning at lower temperature. It is suspected that the enhancement in property is limited by the molecular chain dynamics. Two relaxations were detected in PPTA fiber: one around 250°C and the other around 350°C as introduced above. These two relaxations provide two windows of temperature for post-treatment. One processing window is the temperature ranges from 100 to 350°C and the other is above 350°C but lower than the degradation temperature. The achievable properties of two processing windows are different because the achievable structures are different. Considering the processing temperature between 100 and 350°C, the applied tension is more important than the treatment temperature. The higher the applied tension, the better the orientation and the more perfect the crystal, therefore the higher the modulus. Meanwhile, the treatment temperature and time determine the transverse apparent crystal sizes. Our study shows a trend of decreasing strength with the increasing transverse crystal sizes [17]. Therefore, low temperature, around 180°C, high tensioning and short time are good to achieve strong and relative stiff fiber. In order to achieve super-high modulus, the processing temperature need to be above 350°C and may endure the sacrifice in strength due to thermal degradation.

3.3. Pressure annealing

In order to explore the possibility of new processing

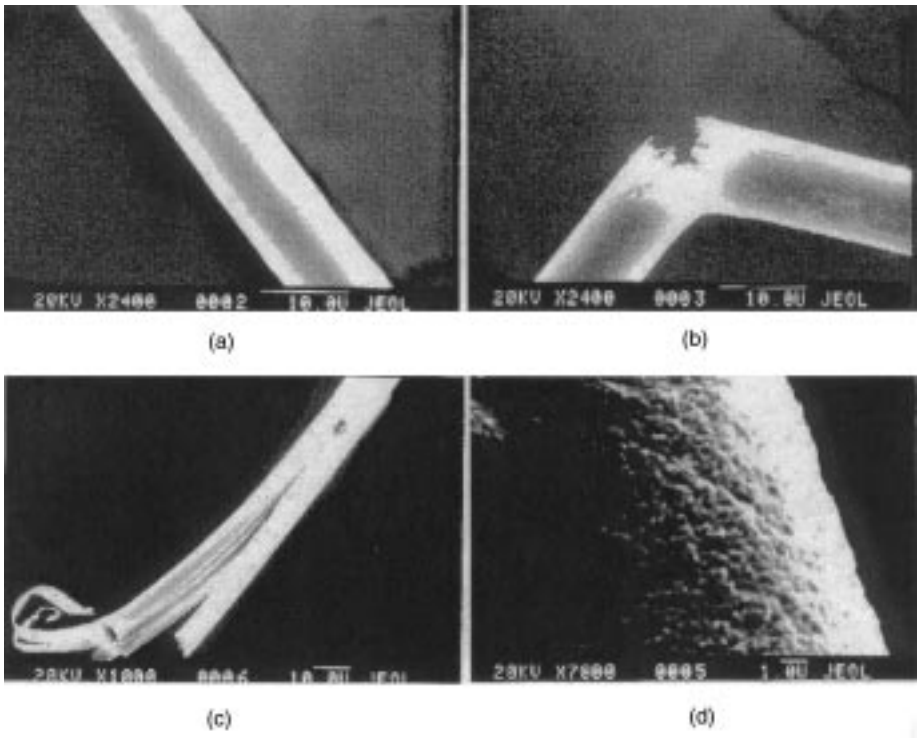

Fig. 17. SEM pictures of a Kevlar® 29 fiber pressure-annealed in Hg: (a) a treated fiber; (b) bending of the treated fiber; (c) a fracture end of the treated fiber; (d) the surface of the treated fiber.

routes and also understand better the structure response to the external stimuli, different pressure annealing experiments were conducted. Pressure annealing, pressure-tensioning, and pressurized steam annealing of Kevlar® 29 fiber were studied. It is shown in Table 3 that the presence of hydrostatic pressure helps to reorient the crystals. The orientation angles of the fibers being treated using different pressurizing media all decrease. Without tensioning, an external hydrostatic pressure of 130 MPa decreases the orientation angle from 13.4 to 8.2° for fibers annealed without pressure. Since the modulus of the fiber is mainly determined by the orientation, it provides a different way other than heat-tensioning to achieve high stiffness.

Our results show that the hydrostatic pressure prevents the change of the crystal structure. The *a*-, *b*-lattice dimensions do not change after the fiber's being pressure annealed, pressure-tensioning annealed and pressurized steam annealed at high temperatures, which is quite different from annealing without pressure. The paracrystalline parameter of the crystal after being pressure-annealed is much bigger than that annealed without pressure at the same temperature. Tensioning along with pressuring helps to decrease the paracrystalline parameter.

In terms of property, the fiber being pressure annealed shows higher modulus than free-length annealing but not as high as those achieved through heat-tensioning. One reason is because the applied hydrostatic pressure is much lower than the applied tension. The change of the structure due to hydrostatic pressure is not difficult to understand. The fiber is highly anisotropic and the transverse modulus of the fiber is much lower than the longitudinal modulus. The hydrostatic pressure causes larger deformation transversely than longitudinally so that the crystal is reoriented by pushing on the crystal transversely instead of stretching the crystal longitudinally. The decrease in the density of the fiber that is usually observed for the change of the crystal structure, which happens in annealing without pressure, is prevented by the hydrostatic pressure. Hence, the change in the crystal structure is relatively small. The densification was observed for the fiber being treated under pressure higher than 100 MPa using mercury as the pressurizing medium. The diameter of the pressure-treated fiber is smaller under optical microscope and SEM (Fig. 17(a)). This needs to be further confirmed by density measurement. In addition, some interaction between mercury and the fiber was observed. It is shown in Fig. 17(b) and (c) that the fiber undergoes a brittle failure and the fracture end of the fiber becomes blunt instead of a generic fibrillar structure, which are common in the failure of PPTA fiber. In addition, a close investigation of the surface of the fiber being Hg-pressure-treated reveals a rich ridge-like feature. (Fig.17(d)) More study needs to be conducted to investigate the possibility of pressure-induced Hg-catalyzed degradation.

The relaxation of the structure is suspected to be associated with the breaking of hydrogen bonds between the bound water and the chain. Water was used as the pressurizing medium to study the role of water in the relaxation. It is found that the presence of saturated water/steam during

annealing prevents the change in the structure. It is shown in Table 3 that, when the fiber was annealed under saturated water at different temperatures, not only the lattice constants remain unchanged but also the transverse apparent crystal sizes and the intensity ratio I_{110}/I_{200}. This convinces us that the pressurized water during annealing suppresses the break of hydrogen bonds and inhibits the conformation change of the chain so as to keep the crystal structure unchanged.

4. Conclusion

From the study of properties and structure of the post-treated Kevlar® fiber, the following were found:

1. Under free-length annealing, the modulus of the fiber slowly decreases with the annealing temperature until 350°C, then drops fast while the strength of the fiber decreases with the annealing temperature and time. The crystal structure of PPTA fiber is not stable and changes with the annealing temperature. The transverse crystal sizes increase with the annealing temperature monotonically. The lattice c-dimension, g_{II}, I_{110}/I_{200}, longitudinal crystal size and equatorial crystallinity show a cooperative change. Their change indicates two relaxations in the crystalline region which is supported by DMTA and TMA measurements. The crystal orientation becomes worse with increasing annealing temperature.
2. Under heat-tensioning, the modulus increases linearly with the applied tension at certain treatment temperature, while the strength remains unchanged. The lattice c-dimension increases largely with the applied tension while the transverse unit cell dimensions and crystal sizes are insensitive to the applied tension. The g_{II} and I_{110}/I_{200} show a cooperative decrease with the applied tension and the crystal orientation improves with increasing applied tension. The deformation of the fiber is due to the elongation and rotation of the crystals.
3. Under pressure annealing, pressure-tensioning annealing and pressurized steam annealing, the modulus increases with the applied pressure and the crystal orientation improves with the applied pressure. Meanwhile, the change of crystal structure under pressure is much smaller than in tension. The presence of pressurized water prevents the structure change. It suggests that the relaxation of the structure is associated with the bound water.

Acknowledgements

We would like to thank the E.I. DuPont Co. (USA) for the financial support for this study through the Center for the University of Massachusetts Research on Polymers (CUMIRP). Helpful discussions with Dr Steve R. Allen (Dupont Co.) are greatly appreciated. Y. Rao thanks Jeremy Morin for his setup of the pressure-tensioning annealing apparatus. We would also like to acknowledge the support from the Materials Research Science and Engineering Center (DMR 9809635) at University of Massachusetts.

References

[1] Kwolek SL. US Pat. 3671542; US Pat. 3,819,587 1972.
[2] Northolt MB, Aartsen JJV. J Polym Sci: Polym Symp 1977;58:283–96.
[3] Barton R. Macromol Sci Phys 1986;B24:119.
[4] Hindeleh AM, Abdo SM. Polym Commun 1989;30:184.
[5] Lee KD, Barton R, Schultz JM. J Polym Sci: Part B: Polym Phys 1995;33:1.
[6] Northolt MG, Aartson JJV. J Polym Sci: Polym Lett Ed 1973;11:333.
[7] Northolt MG. Eur Polym J 1974;10:799.
[8] Watt W, Perov BVE. Strong fibres. New York: North-Holland, 1985.
[9] Panar M, Avakian P, Blumem RC, Gardner KH, Fierke TD, Yang HH. J Polym Sci: Part B: Polym Phys 1983;21:1955.
[10] Wu T, Blackwell J. Macromolecules 1996;29:5621.
[11] Hagege R, Jarrin M, Sotton MJ. J Microsc 1979;113:65.
[12] Riekel C, Eddola A, Heidelbach F, Wagner K. Macromolecules 1997;30:1033.
[13] Dobb MG, Johnson DJ, Saville BP. J Polym Sci: Polym Phys Ed 1977;15:2201.
[14] Wu Z, Zhang A, Cheng SZD. J Polym Sci: Part B: Polym Phys 1990;28:2565–83.
[15] Parimala HV, Vijayan K. J Mater Sci Lett 1993;12:99–101.
[16] Hindeleh AM, Halim NA, Zig KA. J Macromol Sci-Phys 1984;B23:289.
[17] Rao YQ, Waddon AJ, Farris RJ. Polymer 2001;42:5937–46.
[18] Haraguchi K, Kajiyama T, Takayanagi M. J Appl Polym Sci 1979;23:903–14.
[19] Hosemann R, Wilke W. Faserforsch Textiledmik 1964;15:521.
[20] Fukuda M, Kawai H. J Polym Sci: Part B: Polym Phys 1997;35:1423–32.
[21] English AD. Kor Polym J 1996;4:100–6.
[22] Ericksen RH. Polymer 1985;26:733.